

Electron spin resonance in a wide parabolic quantum well

J. D. Caldwell,¹ C. R. Bowers,¹ and G. M. Gusev²¹*Department of Chemistry and National High Magnetic Field Lab, University of Florida, Gainesville, Florida 32611-7200, USA*²*Instituto de Física, Universidade de São Paulo, Caixa Postal 66318, 05315-970, São Paulo, SP, Brazil*

(Received 6 July 2005; published 28 September 2005)

Electron spin resonance spectra were obtained by electrical detection in a remotely Si-doped 400 nm wide GaAs/AlAs digital parabolic quantum well, yielding $g = -0.423$ and $g = -0.405$ in perpendicular and parallel fields of 5 T, respectively. The tilt angle dependence of g in the wide parabolic quantum well is qualitatively different from the previously reported g -factor anisotropy in narrow GaAs quantum wells. The g -factor angle dependence, together with the electrically detected electron-nuclear double resonance spectra, indicate that the spin resonance signals originate mainly from the center of the well. Furthermore, the nuclear spin relaxation in the three-dimensional electron gas (3DES) is found to be independent of temperature in the 1.5–5 K range, while the Korringa law is observed in the 2DES.

DOI: [10.1103/PhysRevB.72.115339](https://doi.org/10.1103/PhysRevB.72.115339)

PACS number(s): 76.70.Dx, 71.18.+y, 71.30.+h, 85.75.-d

Semiconductor nanostructures have been the subject of numerous recent proposals for the realization of spintronics^{1,2} and spin-based quantum information processing devices exploiting electron-nuclear hyperfine couplings.³ The remotely n -doped wide parabolic quantum well (PQW) has several characteristics which make it a model system worthy of further consideration for such applications.⁴ Because the Landé g factor is +1.9 in bulk AlAs^{5–7} and –0.44 in bulk GaAs,⁸ the locally averaged g factor varies along the growth direction (i.e., z axis) in a PQW. Time-resolved Faraday rotation detection of conduction electron spin precession has demonstrated the possibility of g -factor tuning in a PQW via the application of a gate potential.⁹ The confining potential of a wide PQW is broad and shallow, permitting a substantial shift in the electron probability density into the layers of higher Al fraction at a modest gate voltage. The nuclear spin relaxation in these types of structures has also been the subject of a recent theoretical study. Tifrea and Flatté reported calculations demonstrating the ability to tune the nuclear and electronic spin relaxation times via a modification of the electronic local density of states within narrow quantum wells and parabolic quantum wells.¹⁰

At high magnetic fields, rotation of the wide PQW from the perpendicular ($z \parallel B, \theta = 0^\circ$) to the parallel ($z \perp B, \theta = 90^\circ$) orientation causes the energy spectrum to evolve from that of a two-dimensional electron gas (2DES), where

$$E_{i,n}(\theta = 0^\circ) = E_i + \left(n + \frac{1}{2}\right)\hbar\omega_c \quad (1)$$

is the energy of the n th Landau level of the i th subband, to that of a 3DES,⁴ where

$$E(\theta = 90^\circ) = E_i + \frac{\hbar^2 k_x^2}{2m} + \frac{\hbar^2 k_y^2}{2m}. \quad (2)$$

Hence, spin properties such as the g factor and contact hyperfine interaction are expected to reflect the changes in the electronic wave functions when the sample is rotated at a constant applied field. At low fields, the coexistence of the 2DES and 3DES phases has been reported.¹¹

In the perpendicular ($\theta = 0^\circ$) orientation, electrons in each electric subband of the 2DES “sample” the entire PQW structure on a time scale much shorter than the electron Larmor period. In this regime, the g factor of an electron in the i th subband can be calculated from

$$g_i = \frac{\int_{-W_e/2}^{+W_e/2} g(z) |\phi_i(z)|^2 dz}{\int_{-W_e/2}^{+W_e/2} |\phi_i(z)|^2 dz}, \quad (3)$$

where W_e is the effective width of the confining potential, and $\phi_i(z)$ is the subband wave function. Higher i subbands will have increased probability density away from the center of the PQW where the Al fraction is higher. Thus, because of the dependence of the g factor on the Al fraction, the g factor is expected to decrease with increasing i . Figure 1(a) presents a calculation of the effective potential, individual $i=1 \rightarrow 7$ subband electron densities, and total probability density for the 400 nm wide quantum well sample with 7 subbands occupied at zero field. A calculation of g_i based on Eq. (3) for each subband is presented in Fig. 1(b). The calculation predicts a sharp decrease in the g factor for $i=1 \rightarrow 3$. At sufficiently high parallel fields, where the magnetic length $l_0 = \sqrt{\hbar c / eB} \ll W_e$, magnetic confinement dominates, and the electron Zeeman energy is expected to be inhomogeneously broadened due to the distribution of electrons with different g factors.

Electrically detected spin resonance (EDES) and electron-nuclear double resonance (EDENDOR) experiments were performed on a 400 nm wide AlAs/GaAs digital PQW, where the average aluminum mole fraction is 0 at the center and 0.29 at the outer edges. The barriers consist of undoped Al_{0.31}Ga_{0.69}As layers. Electrons are introduced by remote silicon δ -doping. A detailed experimental characterization and theoretical analysis of the transport properties in this particular sample has been published.¹¹ The density and mobility prior to optical illumination with a light-emitting diode (LED) was measured to be $1.5 \times 10^{11} \text{ cm}^{-2}$ and $1.2 \times 10^5 \text{ cm}^2/\text{Vs}$, respectively. Illumination at ~ 1.6 K for 60 s by a LED placed 1 cm away increased these values to $3.5 \times 10^{11} \text{ cm}^{-2}$ and $2.4 \times 10^5 \text{ cm}^2/\text{Vs}$. ESR spectra were ac-

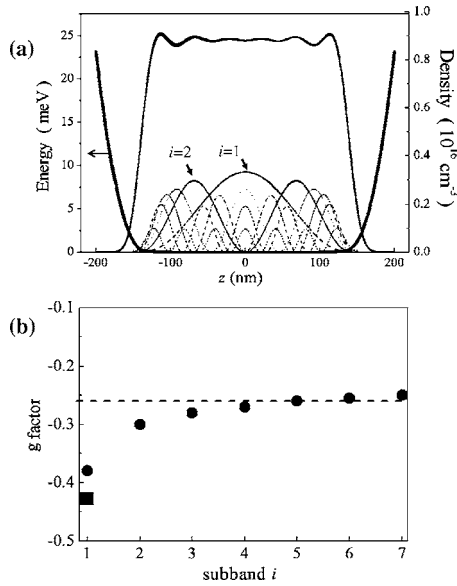


FIG. 1. (a) Calculations of the effective potential energy (bold curve, left axis), total electron density (bold curve, right axis), and individual subband electron densities for $i=1 \rightarrow 7$ (various thin curve types, right axis) in the 400-nm wide parabolic quantum well. (b) Calculated g -factors for each of the individual $i=1 \rightarrow 7$ subbands. The square symbol represents the experimental measurement at a high perpendicular magnetic field.

quired electrically via the resonant change in microwave induced resistance, ΔR_{xx} . The details of the instrumentation and measurement procedure are described in Ref. 12. NMR spectra of nuclei with an appreciable hyperfine coupling to the electron system were acquired via EDENDOR under a steady-state dynamic nuclear polarization (DNP) condition. Additional details of this method will be described below.

The electron g -factor in the PQW was extracted by least squares fitting of the resonant microwave frequency to the measured resonance field position. As shown in previous g -factor studies in GaAs/Al_xGa_{1-x}As square quantum wells and heterostructures, the g -factor in the lowest Landau level exhibits a $g(B) = g_0 - cB$ field dependence.^{13,14} The variation of g_0 and $g(5\text{ T})$ with tilt angle θ is presented in Fig. 2. We find $g = -0.423$ and -0.405 in perpendicular and parallel magnetic fields of 5 T, respectively, a change of about 5%. The temperature dependence of the ESR amplitude (maximum in ΔR_{xx}), linewidth, and line position were also measured in the parallel and perpendicular orientations. The temperature dependence of ΔR_{xx} was found to be much more pronounced in the 2DES in the vicinity of the $\nu=1$ filling factor (FF). The maximum ΔR_{xx} due to ESR was observed at 1.9 ± 0.1 K. No signal was detected above 5 K or below 0.5 K in this orientation. The temperature dependence in the perpendicular orientation was very similar to that observed previously in a square, 30-nm wide Al_{0.1}Ga_{0.9}As/GaAs/Al_{0.1}Ga_{0.9}As well.¹² The FWHM of the ESR resonance, recorded at 4.31 T (corresponding to $\nu=1$) and 1.7 K, was 12 mT. This line width is also comparable to that reported previously for the 30 nm square quantum well.¹² Upon increasing the temperature from 2 to 5 K, the FWHM decreased by about 25%. The linewidth in the par-

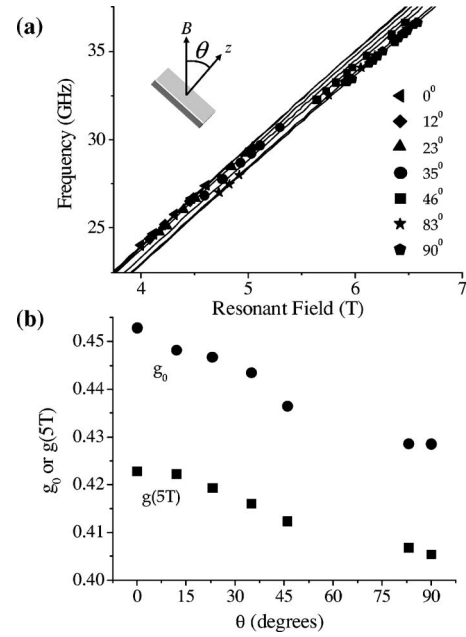


FIG. 2. (a) Dependence of the resonant ESR frequency, ν_{res} , on resonant field, at various tilt angles, θ , as indicated in the legend. The solid curves represent least squares fit to the function $\nu_{\text{res}}(B) = (g_0 + cB)B$. (b) Plots of $g_0(\theta)$ and $g(5\text{ T}, \theta)$.

allel orientation was roughly a factor of 2 greater than in the perpendicular orientation and increased slightly with temperature. The temperature dependence of the resonance field position in the parallel field increased slightly over the 2–10 K range. The shift at 10 K corresponds to a decrease in the g -factor of about 0.6% with respect to the value at 2 K.

To probe the electron-nuclear cross-relaxation and hyperfine coupling and to confirm the sign of the electron g -factor in the 2DES and 3DES states, DNP experiments were conducted at $\theta=0^\circ$ and 90° . In DNP, saturation of the ESR line leads to an enhancement of the local hyperfine field, B_n , yielding an Overhauser shift of the ESR line.^{13,15,16} Depending on the relative signs of the electron g -factor and the nuclear gyromagnetic ratio, B_n may add either constructively or destructively to the applied field. Since the nuclear gyromagnetic ratios of all four isotopes present (²⁷Al, ⁶⁹Ga, ⁷¹Ga, and ⁷⁵As) are positive in sign, B_n adds constructively to the applied magnetic field if $g < 0$. In this case, the ESR resonance can become “pinned” to the applied field, permitting the development of an Overhauser shift which can exceed the resonance linewidth. Hence, the sign of the g factor can be determined unequivocally from the direction of the Overhauser shift in a DNP experiment. In both parallel and perpendicular fields, the ESR is shifted increasingly to lower applied field with decreasing down-sweep rate. This is a clear indication of DNP and confirms that the g factor is indeed negative in both sample orientations.

The overall nuclear spin relaxation time of the PQW nuclei was obtained from the decay of the Overhauser shift following a slow (10 mT/min) DNP down-sweep in the presence of a resonant continuous wave (CW) microwave field.^{17,18} The position of the ESR was followed by 492 mT/

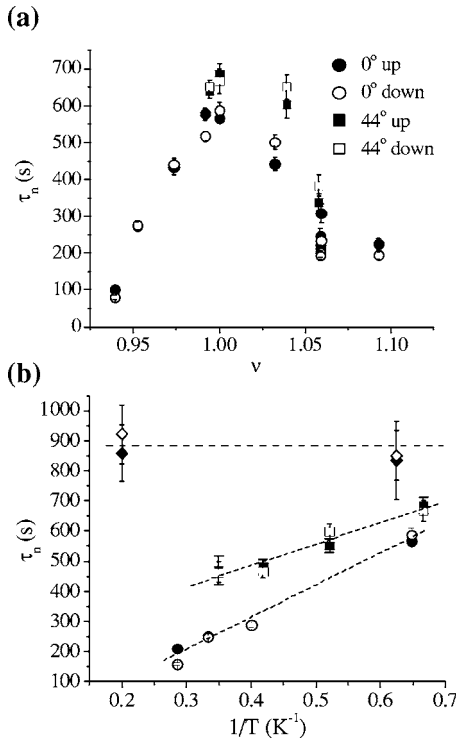


FIG. 3. (a) Landau level filling factor dependence of the Overhauser shift decay constant, τ_n , at $T=1.5$ K, and two different tilt angles: $\theta=0^\circ$ (circles) and 44° (squares). Data acquired in the down- and up-sweeps are displayed as open and filled symbols, respectively. (b) Temperature dependence of τ_n at 0° (circles), 44° (squares), and 90° (diamonds). The data at 0° and 44° were acquired at filling factor $\nu=1$ using microwave frequencies of 27.14 and 35.59 GHz, respectively. The data acquired at 90° was recorded at 36.65 GHz, a frequency which was found to maximize the sensitivity.

min up and down detection sweeps over a small range about the resonance position. This detection sweep rate is too fast to significantly perturb the nuclear spin polarization. The Overhauser shift decay constant was obtained by least squares fitting to a single exponential decay function. The FF dependence of τ_n in the vicinity of $\nu=1$ of the 2DES at two different tilt angles, $\theta=0$ and 44 , is presented in Fig. 3(a). A maximum in τ_n was observed at $\nu=1$ at both angles. Furthermore, τ_n increases with increased θ at all filling factors. In general, the decay constant τ_n includes contributions due to hyperfine relaxation as well as nuclear spin diffusion. The data recorded in the regime of the 2DES are consistent with previous reports of FF dependent magnetoquantum oscillations of τ_n in a 2DES in the quantum Hall regime.^{17,19} The maximum in τ_n is found to occur precisely at $\nu=1$, with the relaxation time dropping sharply on either side of the integer FF. Theoretically, $T_{1n} \rightarrow \infty$ at $\nu=1$. However, in real systems, Landau level overlap due to disorder^{20,21} reduces T_{1n} . The maximum value of $\tau_n=900$ s is in accord with the previous measurements in a narrow GaAs quantum well.¹⁷ In that report, it was suggested that the observed Overhauser shift decay time was probably limited by nuclear spin diffusion into the quantum well (QW) barriers.

The experimental temperature dependence of τ_n in the PQW at $\theta=0^\circ$, 44° , and 90° is presented in Fig. 3(b). Note

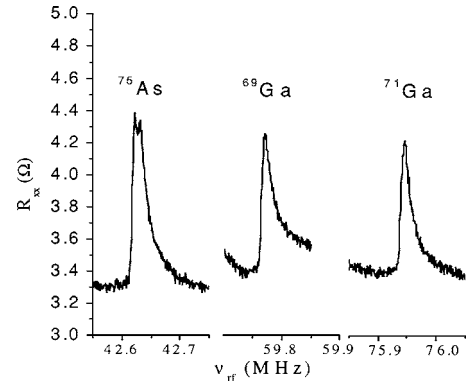


FIG. 4. Electrically detected nuclear magnetic resonance transitions observed at filling factor $\nu=1$ by CW microwave excitation of ESR at a steady state Overhauser shift of 38 mT while sweeping the RF field at a rate of ± 1 kHz/s with a frequency step size of 1 kHz.

that in the parallel field, τ_n is essentially temperature independent, while at both angles within the regime of the 2DES, adherence to the Korringa law ($\tau_n \propto 1/T$) is exhibited. As the sample is rotated toward 90° at a given temperature, an increase in τ_n is observed. It is clear that the change in τ_n is not simply due to a magnetic field dependent relaxation mechanism: the τ_n values measured at 44° and 90° were both recorded at nearly the same applied magnetic field (6.35 and 6.55, respectively), yet τ_n is longer by 30% at $\theta=90^\circ$. The nuclear spin relaxation time of 900 s in the parallel field is significantly longer than in the perpendicular field at temperatures above 1.5 K.

Finally, the delocalization of the electronic wave function across the PQW structure was investigated by electron-nuclear double resonance (ENDOR) spectroscopy. It should be possible to observe an ^{27}Al NMR signal if $\phi(z)$ extends appreciably into the Al containing regions of the PQW. In principle, the relative amplitude of the ^{27}Al signal could be used to evaluate the extent of the electronic delocalization in the PQW. Figure 4 presents the ENDOR spectra of ^{69}Ga , ^{71}Ga , and ^{75}As recorded at a tilt angle of $\theta=16^\circ$ within the $\nu=1$ resistance minimum. The spectra were obtained using a new method in which the radio frequency (RF) is swept while the ESR transition is irradiated at a fixed static magnetic field. Upon sweeping the RF through the nuclear spin resonance condition, the steady state Overhauser shift is perturbed. This is accompanied by a sudden increase in microwave absorption, which reestablishes the steady state DNP condition following the passage through NMR.¹⁶ This new variation of the ENDOR method affords improved sensitivity because it offers the possibility of efficient signal averaging. The FWHM NMR linewidths of the three isotopes were found to be 21, 22, and 30 kHz, respectively. The substantial broadening is likely a consequence of electric quadrupole interactions. This could be associated with the residual strain in the digital AlAs/GaAs superlattice and/or band bending effects. In the case of the ^{75}As resonance, the onset of a splitting is apparent. Repeated attempts to observe a ^{27}Al NMR signal were unsuccessful, even after signal averaging 16 frequency scans, despite the $>25:1$ signal-to-noise (S/N) ratio obtained on the other three isotopes after only a single scan.

To summarize, we have detected the ESR of electrons in a PQW in both the perpendicular and parallel high magnetic fields. The amplitude of the ESR signal was much smaller in the parallel orientation, and the linewidth was greater by about a factor of 2. The temperature dependence of the resistance change due to ESR was much more pronounced in the perpendicular orientation, resembling the temperature dependence in a 30 nm square quantum well. In the parallel orientation, the signal was only weakly temperature dependent, and could be detected at temperatures as high as 10 K.

The g factor was found to be nearly independent of temperature in both orientations, indicating that the charge distribution does not change much in the 0.5–10 K range. A monotonic decrease in the g -factor by $\approx 5\%$ could be induced by rotating the sample from $\theta=0^\circ \rightarrow 90^\circ$ as the system evolves from a 2DES to the equivalent of a 3DES at high fields. At all angles, the observed g -factor is close to that of bulk GaAs, indicating that the ESR signal arises mainly from electrons localized near the center of the PQW where the Al fraction is small. At zero field, seven subbands are occupied, but at $\nu=1$ of the 2DES at high field, only the lowest ($i=1$) subband is occupied. Thus, only this subband, which is resolved energetically from the higher subbands,¹¹ contributes to the resonant microwave photoresistance signal. The observed g -factor is close to the $i=1$ g -factor predicted by Eq. (3), as indicated in Fig. 1(b). The absence of an ^{27}Al NMR signal, despite high signal-to-noise ratios for detection of the other isotopes, is consistent with the g -factor measurements.

The tilt angle dependence $g(\theta)$ in the 400-nm PQW is distinctly different than in the two previous experimental reports of g -factor anisotropy in narrow GaAs/ $\text{Al}_x\text{Ga}_{1-x}\text{As}$ QWs.^{22,23} The time-resolved photoluminescence polarization measurements of Ref. 23 showed no g -factor anisotropy for $W_e \geq 12$ nm, while in an electrically detected ESR study of a 15-nm wide QW,²² g was observed to decrease slightly with increasing θ at $\nu=1$ for small tilt angles. The latter is similar

to the behavior exhibited in Fig. 2 for the 400-nm PQW. As the tilt angle is increased, however, the $g(\theta)$ dependences of the two samples are quite different. For all Landau levels of the 15-nm QW, $g(\theta)$ increases sharply with increasing θ , an effect attributed to nonparabolicity of the bulk GaAs band structure, while in the 400-nm PQW, $g(\theta)$ continues to decrease monotonically. A likely explanation for this observation is as follows: in the wide PQW, where $l_0 \ll W_e$, the detected signal is derived primarily from the central part of the PQW structure where the mobility of the conduction channel is highest. Thus, the $g(\theta)$ dependence in the wide PQW appears to be dominated by the transport characteristics of the 3DES in this sample rather than nonparabolicity effects. The increased broadening of the ESR line observed in the parallel field is consistent with an inhomogeneous distribution of g factors along the z axis of the wide PQW.

The 2DES and 3DES are perhaps most clearly distinguished on the basis of the temperature dependence of the nuclear spin-lattice relaxation times. In the 3DES, a temperature independent decay constant of 900 s was observed, while in the 2DES, the relaxation time was substantially shorter over the temperature range studied, and in addition, the Korringa law was observed. This nuclear spin relaxation behavior reflects differences in the energy spectrum, density of states, electron-electron interactions, and hyperfine interactions. Nuclear spin diffusion will ultimately limit the possibility of obtaining an experimental measurement of the intrinsic nuclear spin-lattice relaxation time due to hyperfine interactions of nuclei in the vicinity of the 3DES.

This work was supported by NSF Grant No. DMR-0106058, CNP/q-NSF U.S.-Brazil Cooperative Research Grant No. 0334573, and the University of Florida. Provision of the digital parabolic quantum well sample by A. I. Toropov and A. K. Bakarov of the Institute of Semiconductor Physics, Novosibirsk, Russia, is gratefully acknowledged.

¹*Semiconductor Spintronics and Quantum Computation*, edited by D. D. Awschalom, D. Loss, and N. Samarth (Springer, Berlin, 2002).

²S. A. Wolf, D. D. Awschalom, A. A. Buhrman, J. M. Daughton, S. von Molnar, M. L. Roukes, A. Y. Chtchelkanova, and D. M. Treger, *Science* **294**, 1488 (2001).

³D. Loss and D. P. DiVincenzo, *Phys. Rev. A* **57**, 120 (1998).

⁴G. M. Gusev, A. A. Quivy, T. E. Lamas, J. R. Leite, A. K. Bakarov, A. I. Toropov, O. Estibals, and J. C. Portal, *Phys. Rev. B* **65**, 205316 (2002).

⁵H. W. van Kesteren, E. C. Cosman, P. Dawson, K. J. Moore, and C. T. Foxon, *Phys. Rev. B* **39**, 13426 (1989).

⁶R. Bottcher, S. Wartewig, R. Bindeman, G. Kuhn, and P. Fischer, *Phys. Status Solidi B* **58**, K23 (1973).

⁷The g factor in a single AlAs quantum well was recently reported to be 1.99 at 34 GHz. See M. Schulte, J. G. S. Lok, G. Denninger, and W. Dietsche, *Phys. Rev. Lett.* **94**, 137601 (2005).

⁸C. Weisbuch and C. Hermann, *Phys. Rev. B* **15**, 816 (1977).

⁹M. Poggio, G. M. Steeves, R. C. Myers, Y. Kato, A. C. Gossard, and D. D. Awschalom, *Phys. Rev. Lett.* **91**, 207602 (2001).

¹⁰I. Tifrea and M. E. Flatte, *Phys. Rev. Lett.* **90**, 237601 (2003).

¹¹C. S. Sergio, G. M. Gusev, J. R. Leite, E. B. Olshanetskii, A. A. Bykov, N. T. Moshegov, A. K. Bakarov, A. I. Toropov, D. K. Maude, O. Estibals, and J. C. Portal, *Phys. Rev. B* **64**, 115314 (2001).

¹²E. Olshanetsky, J. D. Caldwell, M. Pilla, S.-C. Liu, and C. R. Bowers, J. A. Simmons, and J. L. Reno, *Phys. Rev. B* **67**, 165325 (2003).

¹³M. Dobers, K. v. Klitzing, and G. Weimann, *Phys. Rev. B* **38**, 5453 (1988).

¹⁴R. Meisels, I. Kulac, F. Kuchar, and M. Kriechbaum, *Phys. Rev. B* **61**, 5637 (2000).

¹⁵C. Hillman and H. W. Jiang, *Phys. Rev. B* **64**, 201308 (2001).

¹⁶E. Olshanetsky, J. D. Caldwell, A. E. Kovalev, C. R. Bowers, J. A. Simmons, and J. L. Reno, *Physica B* (to be published).

¹⁷A. Berg, M. Dobers, R. R. Gerhardtts, and K. v. Klitzing, *Phys.*

- Rev. Lett. **64** 2563 (1990).
- ¹⁸S. A. Vitkalov, C. R. Bowers, J. A. Simmons, and J. L. Reno, J. Phys.: Condens. Matter **11**, L407 (1999).
- ¹⁹R. Tycko, S. E. Barrett, G. Dabbagh, L. N. Pfeiffer, and K. W. West, Science **268**, 1460 (1995).
- ²⁰I. D. Vagner and T. Maniv, Phys. Rev. Lett. **61**, 1400 (1988).
- ²¹D. Antoniou and A. H. MacDonald, Phys. Rev. B **43**, 11686 (1991).
- ²²M. Döbers, K. v. Klitzing and G. Weimann, Solid State Commun. **70**, 41 (1989).
- ²³P. Le Jeune, D. Robart, X. Marie, T. Amand, M. Brousseau, J. Barrau, V. Kalevich, and D. Rodichev, Semicond. Sci. Technol. **12**, 380 (1997).